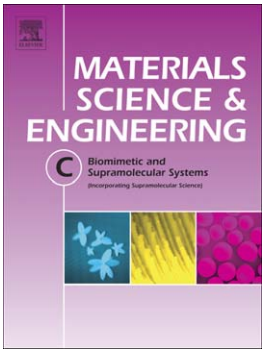

Wetspun poly-L-(lactic acid)-borosilicate bioactive glass scaffolds for guided bone regeneration

João S. Fernandes, Rui L. Reis, Ricardo A. Pires

PII: S0928-4931(16)31652-6
DOI: doi:10.1016/j.msec.2016.10.007
Reference: MSC 6976

To appear in: *Materials Science & Engineering C*

Received date: 4 April 2016
Revised date: 1 September 2016
Accepted date: 7 October 2016

Please cite this article as: João S. Fernandes, Rui L. Reis, Ricardo A. Pires, Wetspun poly-L-(lactic acid)-borosilicate bioactive glass scaffolds for guided bone regeneration, *Materials Science & Engineering C* (2016), doi:10.1016/j.msec.2016.10.007

Wetspun Poly-L-(Lactic Acid)-Borosilicate Bioactive Glass Scaffolds for Guided Bone Regeneration

João S. Fernandes[1,2*], Rui L. Reis[1,2], Ricardo A. Pires[1,2*]

[1] 3B's Research Group - Biomaterials, Biodegradables and Biomimetics, University of Minho, Headquarters of the European Institute of Excellence on Tissue Engineering and Regenerative Medicine, AvePark-Parque de Ciência e Tecnologia, Zona Industrial da Gandra, 4805-017 Barco GMR, Portugal

[2] ICVS/3B's - PT Government Associate Laboratory, Braga/Guimarães, Portugal

* Corresponding Authors:

Ricardo A. Pires. E-mail: rpires@dep.uminho.pt

Tel: +351 253 510 907

Fax: +351 253 510 909

João S. Fernandes. E-mail: joao.fernandes@dep.uminho.pt

Tel: +351 253 510 900

Fax: +351 253 510 909

Abstract

We developed a porous Poly-L-Lactic Acid (PLLA) scaffold compounded with borosilicate bioactive glasses (BBGs) endowing it with bioactive properties. Porous PLLA-BBGs fibre mesh scaffolds were successfully prepared by the combination of wet spinning and fibre bonding techniques. Micro-computed tomography (μCT) confirmed that the PLLA-BBG scaffolds containing ≈ 25% of BBGs (w/w) exhibited randomly interconnected porous (58 to 62% of interconnectivity and 53 to 67% of porosity) with mean pore diameters higher that 100 μm. Bioactivity and degradation studies were performed by immersing the scaffolds in simulated body fluid (SBF) and ultrapure water, respectively. The PLLA-BBG scaffolds presented a faster degradation rate with a constant release of inorganic species, which are capable to produce calcium phosphate structures at the surface of the material after 7 days of immersion in SBF (Ca/P ratio of ~1.7). Cellular *in vitro* studies with human osteosarcoma cell line (Saos-2) and human adipose-derived stem cells (hASCs) showed that PLLA-BBGs are not cytotoxic to cells, while demonstrating their capacity to promote cell adhesion and proliferation. Overall, we showed that the proposed scaffolds present a tailored kinetics on the release of inorganic species and controlled biological response under conditions that mimic the bone physiological environment.

Keywords: Poly-L-Lactic Acid, borosilicate bioactive glasses, bioactivity, scaffold, interconnected porosity

1. Introduction

Bone has a remarkable auto-regenerative capacity; however, when a large defect is generated, by accident or disease, it cannot regenerate the lost tissue by itself. At present, both autogenic and allogenic transplants have been used for bone repair, but with different limitations, namely: the autogenic strategy is restricted in supply and limited by the size of the defect; while the allogenic one may present incompatibility and a high risk of infection and of transplant rejection [1, 2]. In this context, bone tissue engineering is a promising approach that provides a strategy based on the use of biodegradable porous scaffolds that serves as a support and mimics of the bone extracellular matrix (ECM), which promotes cell attachment and proliferation. The matching of the scaffolds degradation kinetics with the timeframe of the cellular regenerative processes, allows the formation of new bone while the scaffolds are degraded [3-5].

Numerous biomaterials have been developed based on natural and synthetic biodegradable polymers or bioactive ceramics [6-12]. Synthetic materials present limited variability allowing the optimisation of the scaffold's properties (e.g. porosity and degradation) to promote cell adhesion and proliferation, as well as the capacity to induce the formation of new bone. Poly-L-Lactic Acid (PLLA) is one of such polymers: it is biodegradable and has been accepted in different medical devices by the US Federal Food and Drug Administration (FDA), which makes it highly attractive for biomedical applications. Furthermore, PLLA is a biocompatible material, which can be manufactured through various techniques [13-17]. On the other hand, inorganic materials, e.g. silicate-based bioactive glasses (BG), hydroxyapatite and tricalcium phosphates, have been widely studied due to their reported bioactivity, osteoconductivity, and ability to directly bond to bone; as well as improving cell

adhesion, proliferation and differentiation [18-22]. Moreover, some inorganic materials (e.g. composed by Si, B, Sr, Ca, Mg or Zn) are reported to have a part in bone metabolism, osteo- and angiogenesis, cell proliferation, as well as, presenting antibacterial properties [18, 23-26].

Hitherto no single material has all the essential attributes required for an ideal scaffold for bone tissue engineering. Therefore, there is a rising interest in three-dimensional (3D) scaffolds that can combine the bioresorbability of the polymer with the bioactivity of glass/ceramic phases, resulting in a material that combines all the properties that were previously described. Herein we propose a composite system of PLLA-borosilicate bioactive glass (PLLA-BBG) that provides a structural support for cellular attachment and proliferation, leading to the engineering of bone tissue that combine its chemical, biochemical and biological properties. PLLA as a slow degradation rate that makes it a more suitable material for bone regeneration, in which the healing times are longer. Moreover, it degrades into lactic acid, which can be subsequently secreted as carbon dioxide by entering the Krebs cycle. While, the composite fillers (i.e. BBGs) might be able to improve its mechanical properties, they can control the acidity of the surrounding tissue (generated by the inflammatory process that precedes tissue regeneration) during its degradation. The release of glass modifier cations from the BBGs, can be used by the surrounding cellular environment to produce a phosphated mineral phase, which is essential to create a strong interfacial adhesion between the scaffold and bone [5]. Wet spinning methodology allows the fabrication of complex 3D structures with controlled properties such as, porosity, pore structure and interconnectivity, influencing: cell adhesion, proliferation and vascularisation trough the scaffold [27, 28]. In wet spinning, the polymer dissolved in a suitable solvent is extruded into a liquid that is miscible with the spinning solvent but a non-solvent of the

polymer. This results in to solvent removal and fibres precipitation. Unlike electrospinning, wet spinning is able to create macro to micro-scale fibres allowing cell penetration through the scaffold for bone regeneration and vascularisation. The required pore size might differ between cell types [29], however, numerous studies support that the optimal pore size for regeneration and mineralisation of bone ranges from 100 to 300µm [30, 31]. Recent studies of the effect of porosity on the ingrowth of MC3T3-E1 pre-osteoblastic cells into 3D scaffolds reported a suitable cellular response within this range [32].

In this context, we compounded PLLA-BBG into fibrous scaffolds (25% w/w of BBGs), where the BBGs were formulated with different divalent modifier cations (i.e. Ca^{2+}, Mg^{2+} and Sr^{2+}), and tested them for their biodegradability, bioactivity and biological response using human osteosarcoma cell line (Saos-2) and human adipose-derived stem cells (hASCs).

2. Experimental

2.1 Materials

All chemicals used for the glass synthesis were reagent grade: boron oxide (Alfa Aesar, Germany), calcium carbonate (Sigma-Aldrich, Portugal), sodium bicarbonate (Sigma-Aldrich, Australia), silica gel 60M (Macherey-Nagel, Germany), magnesium oxide (Sigma-Aldrich, Portugal) and strontium carbonate (Sigma-Aldrich, Australia). PLLA (with a L-lactide content of 99.6% and an average M_w of 69 000 $g.mol^{-1}$, from Cargill Dow LLC, USA) was used to produce the desired fibre meshes.

BBGs were produced by mixing appropriate amounts of SiO_2, B_2O_3, $NaHCO_3$, and $CaCO_3$, or MgO, or $SrCO_3$ on an agate mortar with ethanol. Upon drying, the mixture was heated to 1450 ºC on air for 1 hour. Afterwards, the melt was quickly poured into a

water bath maintained at 4 ºC to form a glass frit. The glasses, of general formula $0.05Na_2O \cdot xMgO \cdot yCaO \cdot (0.35\text{-}x\text{-}y)SrO \cdot 0.20B_2O_3 \cdot 0.40SiO_2$ (molar ratio, where x, y = 0.35 or 0.00, and $x \neq y$), were ground in an Agate mortar (RETSCH, Germany) to obtain microparticles and, afterwards, sieved to a size smaller than 63 μm. The density of the BBGs was measured using a Multi pycnometer (Quantachrome Instruments, USA) with helium at 110 °C using ≈ 5 g of each sample.

2.2. Preparation of wet-spun fibre mesh scaffolds

PLLA-BBG fibres were fabricated through the wet spinning of a PLLA solution containing a homogeneous suspension of BBG particles. These fibres were transformed into circular shape fibre mesh scaffolds by fibre bonding. Three different PLLA-BBG scaffolds were fabricated (PLLA-BBG-Mg, PLLA-BBG-Ca and PLLA-BBG-Sr) using three different BBGs (BBG-Mg, BBG-Ca and BBG-Sr, that present, respectively, Mg, Ca and Sr as divalent modifier cations). Unfilled PLLA scaffolds were used as control.

2.2.1. Wet spinning

After preparing a PLLA solution in chloroform (30% w/v), BBGs (25% BBG/PLLA w/w) were added under constant stirring to avoid the agglomeration of BBG particles. Subsequently, the PLLA-BBG solution was wet spun thought a syringe equipped with a 25 G needle with the tip cut horizontally and perpendicular to the flow. The fibres were extruded at a rate of 15 ml/h into a coagulation bath of methanol. Finally, fibres were collected and dried overnight on the fume hood at room temperature.

2.2.2. Fibre bonding

To fabricate the PLLA-BBG fibre mesh scaffolds, fibres (≈ 80 mg) were first pre-moulded into a 20 mm diameter metal mould and bonded at 147 °C with a 5 kg weight

on the top for 6 min. The fibre bonding temperature was optimised with the help of differential scanning calorimetry analysis (DSC) of PLLA (T_g of 56.7 °C and a T_m of 165.4 °C). Finally, a 6 mm puncture was used to obtain specimens of 6 mm diameter and 0.5 mm height.

2.3. *In vitro* characterisation of wet-spun fibre mesh scaffolds

2.3.1. Differential scanning calorimetry (DSC) analysis

The glass transition (T_g) and melting (T_m) temperatures of the PLLA were determined by differential scanning calorimetry (DSC, TA Instrument Q100 calorimeter, USA), using a double run between -40 to 200 °C (first run to determine T_g and to remove thermal history, and second run to determine T_m), at a heating and cooling rates of 10 °C/min under nitrogen atmosphere, using ~8 mg of sample.

2.3.2. Scanning electron microscopy (SEM)

Scanning Electron Microscopy (Leica Cambridge S360, equipped with an energy dispersive X-ray spectrometer link-eXL-II, UK) was used to assess the surface morphology of the PLLA-BBG scaffolds, as well as to monitor the deposition of calcium phosphate structures on the surface of the fibres after 7 and 14 days of immersion in Simulated Body Fluid (SBF).[33] All the PLLA-BBG scaffolds were sputter-coated (Fisons Instruments SC502, UK) with gold before the analysis. All the micrographs were acquired using a beam energy of 5.0kV and a working distance (WD) of ≈5.2 mm.

2.3.3. X-ray diffraction analysis (XRD)

The PLLA-BBG scaffolds were analysed before and after 7 and 14 days of immersion in SBF by X-ray diffraction (XRD, Bruker D8 Discover, Germany), using Cu radiation

at a wavelength of 1.5406 Å at 40 kV and 40 mA, with a step size of 0.02 ° in a 2θ range between 5 ° to 50 ° and a scanning speed of 1 s/step. The crystalline patterns were identified by comparison with the data listed in the Joint Commission on Powder Diffraction Standards (JCPDS).

2.3.4. Micro-computed tomography (μCT)

Three samples from each PLLA-BBG and PLLA scaffolds were analysed by micro-computed tomography (μCT) using a high-resolution μ-CT scanner (Skyscan 1072, Kontich, Belgium), a pixel size of 6 μm and integration time of 1.7 ms. The X-ray source was set at 43 kV of energy and 234 μA of current. Approximately 400 projections were acquired over a rotation range of 180°, with a rotation step of 0.45°. Data sets were reconstructed using standardised cone-beam reconstruction software (NRecon v1.4.3, SkyScan). The output format for each sample was 400 serial 1024 × 1024 bitmap images. Representative data sets were segmented into binary images using a dynamic threshold of 40-150 for the polymer (blue images, **Figure *2***) and 150-255 for BBGs (red images, **Figure *2***). These representative data sets were used for morphometric 3D analysis (CT Analyser, v1.5.1.5, SkyScan) and to build 3D models (ANT 3D creator, v2.4, SkyScan). The morphometric analysis included porosity, mean wall thickness, mean pore diameter and pore interconnectivity. 3D virtual models of representative regions in the bulk of the scaffolds were created, visualised, and registered using image processing software (CT Analyser and ANT 3D creator).

2.3.5. Bioactivity assay

SBF was produced in accordance with the procedure of Kokubo et al [33]. Triplicate samples of the PLLA-BBG scaffolds, were immersed in SBF at a ratio of 10:10 [PLLA-BBG scaffolds (mg): SBF (mL)] and incubated for 7 and 14 days in an oven maintained

at 37 °C. After each time point samples of PLLA-BBG scaffold were collected and dried at 37 ºC in order to obtain the XRD patterns and SEM micrographs. Each immersion solution was filtered and analysed by inductive coupled plasma (ICP, Horiba, Japan) to determine the corresponding Ca and P concentrations present in the solution at each time point. The ICP absorption was measure at specific wavelengths (λ= 393.366 nm for Ca; λ=213.62 nm for P) and the Ca and P concentrations were determined using calibration curves previously obtained with standard solutions (Alfa Aesar).

2.3.6. Degradation assay

The PLLA-BBG scaffolds (n=3 per time point) were immersed in ultrapure water at a ratio of 10:10 [PLLA-BBG scaffolds (mg): water (mL)] for 7, 14, 21, 28, 60 and 90 days in a water-shaking bath at 60 rpm and 37°C. Each immersion solution was filtered and their respective pH was measured. ICP analysis was performed to determine the Si, B, Ca, Mg and Sr concentrations in the immersion solutions. The absorption was measure at specific wavelengths (λ= 251.611 nm for Si, λ= 249.773 nm for B, λ= 393.366 nm for Ca, λ= 407.771 nm for Sr and λ= 279.553 nm for Mg) and their concentrations were determined using calibration curves previously obtained with standard solutions (Alfa Aesar).

The PLLA-BBG scaffolds were removed from the immersion solution, the excess surface water was removed and the samples were immediately weighed. Afterwards, the samples were dried in the oven at 37 °C, to constant weight, recording the final mass of each specimen. The water uptake (WU) was calculated according to Eq. (1):

$$WU(\%) = \left(m_{tp} - m_f\right)/m_f \times 100 \qquad \text{Eq. (1)}$$

Where m_{tp} is the wet mass of the specimen at the specific time (days), and m_f is the final mass after immersion and drying. The weight loss (WL) was calculated according to Eq. (2):

$$WL(\%) = \left(m_f - m_i\right)/m_i \times 100 \qquad \text{Eq. (2)}$$

Where m_f is the mass of the dried specimen after its immersion in water, and m_i is the mass of the dried specimen before immersion in water.

Thermogravimetric analysis (TGA) was used to determine the amount of BBGs incorporated in the PLLA-BBGs composites and to monitor changes in the weight (mass) of the inorganic BBGs present in the scaffolds as a function of degradation process. TGA thermograms were obtained using a TGA Q500 series (TA Instruments, USA). Experiments were performed in platinum pans, at a heating rate of 40 °C/min from 50 °C to 700 °C under oxygen atmosphere.

2.4. Cytotoxicity evaluation

The cytotoxicity assessment was performed by culturing Saos-2 cells in the presence of the PLLA-BBG scaffolds. Cells were expanded in Dulbecco's Modified Eagle Medium (Sigma, USA) supplemented with 10% heat-inactivated foetal bovine serum (FBS, Alfagene, USA) and 1% antibiotic/antimycotic solution (100 U/mL penicillin and 100 μg/mL streptomycin; Alfagene, USA). Cells were cultured at 37 °C in an atmosphere of 5% CO_2. Confluent Saos-2 cells between passages 13 and 17 were harvested and seeded onto the bottom of 24-well plates at a density of 2×10^4 cells/well before put in contact with scaffolds. The Saos-2 cells cultured in the presence of PLLA and absence of glass particles were used as negative control and latex (6 mm discs) were used as positive control.

The metabolic activity and cellular proliferation of the Saos-2 cells were monitored at 1, 3 and 7 days by MTS (3-(4,5-dimethylthiazol-2-yl)-5-(3-carboxymethoxyphenyl)-2-(4-sulfophenyl)-2 H-tetrazolium – Promega, UK) and PicoGreen® (Quant-iT™ PicoGreen® dsDNA Assay Kit – Invitrogen, USA), respectively, following the supplier's instructions.

2.5. Cell adhesion experiments

The cell adhesion study was performed with hASCs. The hASCs cells were isolated from human subcutaneous adipose tissue samples obtained from lipoaspiration procedures performed on women with ages between 35 and 50 years old (under a protocol previously established with the Department of Plastic Surgery of Hospital da Prelada in Porto, Portugal) and frozen at -80 °C. The cells were grown in a culture medium consisting of αMEM, 10% FBS and 1% of antibiotic-antimycotic mixture. When an adequate cell number was obtained (P3), cells were detached with trypsin/EDTA and seeded at a density of 3×10^4 cells onto the surface of each scaffold. After 24 h of cell attachment, cell-constructs were placed in new 24-well plates and 1 mL of basal medium was added to each well. The basal culture medium consisted of αMEM (Gibco, UK) supplemented with 10% FBS and 1% antibiotic/antimycotic solution (final concentration of penicillin 100 units/mL and streptomycin 100 mg/mL). The cell-constructs were cultured for 7 and 21 days in a humidified atmosphere at 37 °C, containing 5% CO_2. The culture medium was changed every 2–3 days until the end of the experiment. The metabolic activity and cellular proliferation were monitored at 7 and 21 days by MTS (3-(4,5-dimethylthiazol-2-yl)-5-(3-carboxymethoxyphenyl)-2-(4-sulfophenyl)-2 H-tetrazolium – Promega, UK) and PicoGreen® (Quant-iT™ PicoGreen® dsDNA Assay Kit – Invitrogen, USA), respectively, following the supplier's instructions.

Cell morphology was also evaluated at 7 and 21 days; cells were washed twice with phosphate buffer saline (PBS) and then fixed with Formalin for 15 min at room temperature. Prior to the analysis by SEM (Leica Cambridge S360, UK) equipped with an energy dispersive spectrometer (EDS; link-eXL-II), the samples were sputter coated (Fisons Instruments SC502, UK) with gold or carbon.

3. Results and Discussion

Silicate-based bioactive glass particles have been reported to improve the bioactive performance of scaffolds for tissue engineering [34, 35], as well as, stimulating the proliferation and differentiation of cells [4, 18]. Herein, we evaluated the impact of borosilicate-based glasses (presenting different divalent modifier cations, i.e. Mg^{2+}, Ca^{2+} and Sr^{2+}) on the degradation and bioactivity of wet-spun PLLA-BBG composites, as well as, their cytotoxicity towards Saos-2 and hASCs and the adhesion and proliferation of hASCs cultured onto the scaffolds.

3.1. Characterisation of wet-spun fibre mesh scaffolds

PLLA-BBG fibres were produced using a solution of PLLA in chloroform to which the synthesised BBGs (<63 μm and density of ~2.8 $g.cm^{-3}$) were suspended. Upon injection of this suspension into a methanolic coagulation bath the fibres were dried and moulded by fibre bonding. Scaffold specimens were prepared as 6 mm diameter discs (using a puncture), sterilised (88% CO_2 and 12% ethylene oxide at 45 °C with 180 kPa and 55% of humidity for 10 h) and preserved in a desiccator. **Figure *1*** presents the SEM images and X-ray diffraction patterns of the PLLA-BBG scaffolds.

[Figure 1]

Figure 1. *SEM micrographs with insets of BBG particles incorporated into the fibres (a, b, c and d) and X-ray diffraction patterns (e) of PLLA and PLLA-BBG scaffolds (PLLA-BBG-Mg, PLLA-BBG-Ca and PLLA-BBG-Sr).*

The XRD patterns of the scaffolds exhibited the characteristic peaks of PLLA at 2θ = 12.5 °, 14.7 °, 16.6 °, 19.1° and 22.3°, while there are no detectable peaks of BBGs due to their amorphous state and low concentration at the scaffold surface [36].

The morphological analysis of the PLLA and PLLA-BBGs scaffolds was executed by μ-CT (**Figure *2***). We observed the typical fibre mesh structure with random porous distribution, which are vital for cell ingrowth [27, 37], as well as a homogenous dispersion of BBGs all over the scaffolds. From the mathematical analysis of the data (performed by the CTAn software, Table 1) it is possible to determine the porosity, interconnectivity and thickness of the scaffolds. These properties were unchanged with the incorporation of BBGs. The whole set of scaffolds presented porosities ranging from 53 to 67% and interconnectivity between 58 and 62%. It is also relevant to point out that the mean pore diameters are >100 μm, within the range of optimal pore size for cell penetration, regeneration and mineralisation of bone [27, 38]. Therefore, combining wet spinning and fibre bonding we were able to prepare PLLA-BBGs scaffolds with morphological characteristics appropriate for cell colonization.

[Figure 2]

Figure 2. *Representative μCT cross-sections of the PLLA and PLLA-BBGs scaffolds. The upper images combine the PLLA fibres (blue) and the distribution of the BBGs (red), while the bottom images represent only the distribution of BBG particles (red) within the scaffold.*

Table 1. *Porosity, mean pore diameter and interconnectivity of the scaffolds determined by μCT*

Samples	Porosity (%)*	Mean pore diameter (μm)*	Interconnectivity (%)*
PLLA	64.57 ± 7	117.41 ± 7	57.53 ± 4
PLLA-BBG-Mg	53.39 ± 2	148.77 ± 6	57.80 ± 5
PLLA-BBG-Ca	66.75 ± 2	111.65 ± 6	61.55 ± 6
PLLA-BBG-Sr	63.53 ± 5	126.17 ± 6	58.91 ± 3

* No statistically significant differences were detected.

3.2. *In vitro* degradation and bioactivity

The WL and WU are strongly correlated with the water stability and biodegradability of the scaffolds. They are extremely relevant properties to determine their expected lifetime under the physiological environment [39]. The WL (**Figure *3***a) data shows a faster degradation rate for the PLLA-BBGs compared to PLLA over 30 days of immersion in ultrapure water (e.g. at day 30, the PLLA-BBGs' WL is ~15% higher than the PLLA's WL). This data clearly suggests that the addition of BBG particles to the scaffolds augments its biodegradability, reflected in the increase of the WL of the composites [6, 40].

In the case of the WU (**Figure *3***b), while the PLLA scaffolds uptake a constant amount of water throughout the tested time period (i.e. ~15%), the PLLA-BBGs scaffolds present a WU peak at day 7 (similar to the PLLA WU) followed by a subsequent reduction over the immersion time. This latter reduction is probably associated with the increase of the local concentrations of inorganic species leached from the glass that, subsequently, at the latter time point, deposit in the surface of the glass particles,

limiting the exchange of water between the immersion solution and the inorganic portion of the composites.

The release profile of inorganic species (**Figure *3***c, data obtained by ICP) showed a continuous release of B, Si, Ca/Sr/Mg–related species over the tested timeframe. This was accompanied with an increase of the solution pH (from ≈6 to ≈9.6 over 30 days), which might be critical to balance the pH decrease generated by the inflammatory process that precedes tissue regeneration of the implanted scaffold. There was a higher release rate in the case of PLLA-BBG-Mg scaffolds, which can be related with the relatively smaller size of Mg^{2+} (when compared with Ca^{2+} and Sr^{2+}) that enhance its diffusion from the glass particles to the surrounding medium. This was also confirmed by TGA where we detected a larger reduction of the glass percentage in the composites containing BBG-Mg after 30 days of immersion (from ~24% to ~18%).

[Figure 3]

Figure 3. *WL (a), WU (b) and release profile of chemical species (c) of the PLLA and PLLA-BBG scaffolds over 30 day of immersion in ultrapure water at 37 ºC.*

Typically, a bioactive material should promote the formation of a calcium phosphate layer on its surface upon immersion in SBF [41]. In **[Figure 4]**

Figure 4 we present the SEM images and the XRD patterns of the PLLA and PLLA-BBGs after immersion in SBF for 0, 7 and 14 days. The SEM images clearly demonstrate the deposition of an apatite-like layer in the surface of the composites, namely close to the glass particles, after 7 and 14 days of immersion in SBF. These layers present a cauliflower morphology, which is the characteristic shape of apatite structures, including hydroxyapatite [42, 43]. Furthermore, the EDS analysis executed on the regions where the inorganic deposits were observed indicate Ca/P ratios of ~1.5

for day 7 and ~1.7 for day 14, which is close to the typical apatite Ca/P ratio of 1.67 [44]. In addition, the ICP quantification of the Ca and P present in the SBF as a function of time corroborates this findings, revealing a fast deposition of phosphates onto the surface of the PLLA-BBG scaffolds which might be related with the initial formation of amorphous calcium phosphates and, afterwards, to their evolution to a crystalline phase [45]. Nevertheless, in the case of the PLLA scaffolds (**[Figure 4]**

Figure 4a, used as controls), the SEM micrographs do not show any deposition of inorganic layers at the surface of the scaffolds.

The XRD patterns of the PLLA-BBG scaffolds after 7 and 14 days of immersion in SBF presented characteristic peaks of crystalline phosphate structures (2θ = 28.9 º and 2θ = 25.8 º), while there are no peaks observed for the PLLA scaffolds [46, 47]. The peak 2θ = 28.9 º, which appeared in all PLLA-BBG scaffolds (**[Figure 4]**

Figure 4b, 4c and 4d), is commonly attributed to hydroxyapatite structures [47]. To emphasise, PLLA-BBG-Ca scaffolds (**[Figure 4]**

Figure 4c) presented a ~5 times higher peak (2θ = 28.9 º) at day 14 of immersion comparing with other two scaffolds, PLLA-BBG-Mg and PLLA-BBG-Sr (**[Figure 4]**

Figure 4c in relation to **[Figure 4]**

Figure 4a and **[Figure 4]**

Figure 4d, respectively). This observation is indicates that the higher concentration of Ca^{2+} cations (from the SBF and leached from the BBG-Ca glass particles) promotes an increase on the formation of calcium phosphate crystalline structures on the surface of the scaffolds. The peak at 2θ = 28.9 º can also be attributed to tricalcium phosphate (i.e. $Ca_3(PO_4)_2$).[48] Regarding the PLLA-BBG-Mg scaffolds, the same peak (2θ = 28.9 º) is

found, but with lower intensity, which can be also related with the formation of magnesium phosphate crystalline structures (i.e. $Mg_3(PO_4)_2$) [49]. The peaks at 2θ = 25.4 º and 2θ = 28.9 º are also present in the PLLA-BBG-Sr XRD pattern, however, they are with lower intensity than the ones recorded for the PLLA-BBG-Ca (**Figure 4**d and 4c, respectively). These two peaks are commonly associated with the formation of apatite structures [47, 50]. In the specific case of the peak at 2θ = 25.4 º, it is usually associated with apatite structures where calcium is substituted by strontium [46]. The lower intensity of the peaks may be due to the fact that the Sr^{2+} cations affect the adsorption of Ca^{2+} in the initial stages of apatite formation [51]. Those two peaks are also found in the strontium phosphate crystalline phases, such as $SrHPO_4$ [52]. Overall, the XRD data is consistent with the deposition of Ca/Mg/Sr phosphates on the surface of the PLLA-BBGs scaffolds, that subsequently evolve to form different crystalline phases until it forms an hydroxyapatite-like surface layer with their characteristic cauliflower morphology.

[Figure 4]

Figure 4. *XRD patterns and SEM micrographs of (a) PLLA, (b) PLLA-BBG-Mg, (c) PLLA-BBG-Ca, and (d) PLLA-BBG-Sr, after 7 and 14 days of immersion in SBF at 37 ºC.*

3.3. *In vitro* cytotoxicity

The PLLA and PLLA-BBGs scaffolds were tested for their *in vitro* cytotoxicity. To this purpose, we evaluated the metabolic activity and cell proliferation of Saos-2 cells cultured in direct contact with the scaffolds for 7 days (**Figure *5***a). Under these experimental conditions, neither PLLA nor PLLA-BBG scaffolds induced a significant reduction of the cellular metabolic activity. DNA quantification (Figure 5b) presents a

similar profile, indicating that a similar amount of DNA was detected when the cells were in contact with PLLA and PLLA-BBG scaffolds. In conjunction the metabolic activity and DNA quantification data revealed that the presence of the BBGs particles did not induce any significant differences in cell proliferation, demonstrating that the incorporation of BBGs did not elicit any cytotoxic effects.

[Figure 5]

Figure 5. *MTS (a) and DNA (b) quantification data of Saos-2 cells cultured in direct contact with PLLA and PLLA-BBG scaffolds during 1, 3 and 7 days. Latex discs were used as positive control and standard culture medium was used as negative control. The data was obtained from at least 3 independent experiments and is expressed as mean ± SD. The data was analysed by non-parametric statistics: Kruskal-Wallis test ($p<0.001$), followed by a Dunn's Multiple Comparison test.* ****Extremely significant ($p<0.001$);* ***Very significant ($0.001<p<0.01$);* **Significant ($0.01<p<0.05$).*

3.3. Cell adhesion assay

hASCs are widely studied for bone tissue engineering due to their high abundance in fat tissue, ease to harvest and proliferate and, specially, because they present a high percentage of their population with an osteogenic potential [53, 54]. The cell adhesion assay was used to evaluate the suitability of the PLLA-BBG scaffolds for guided bone regeneration. hASCs were directly seeded on the top of the scaffolds (PLLA and PLLA-BBGs) and their morphology and ability to proliferate were assessed by SEM (Figure 6a through 6h), MTS and DNA quantification (**Figure *6***i and **Figure *6***j, respectively).

[Figure 6]

Figure 6. *Adhesion and proliferation study of the hASCs cultured on PLLA and PLLA-BBG scaffolds analysed by SEM after 21 days of cell culture: (a) PLLA, (b) PLLA-BBG-Mg, (c) PLLA-BBG-Ca and (d) PLLA-BBG-Sr. Cross-sections of (e) PLLA, (f) PLLA-BBG-Mg, (g) PLLA-BBG-Ca and (h) PLLA-BBG-Sr scaffolds are presented to evaluate the capacity of the hASCs to colonize the interior of the scaffolds. Red circles show cell that are driving from the top layer to the interior of the scaffolds. (i) MTS and (j) DNA quantification executed after 7 and 21 days of hASC cell culture. Standard culture medium was used as negative control. The metabolic activity and cell proliferation data is expressed as mean ± SD. The data was analysed by non-parametric statistics: Kruskal-Wallis test ($p<0.001$), followed by a Dunn's Multiple Comparison test. ***Extremely significant ($p<0.001$); **Very significant ($0.001<p<0.01$); *Significant ($0.01<p<0.05$).*

The SEM micrographs show that cells were able to attach and spread on the surface of all the scaffolds, as well as to penetrate through their pores (Please see red circles, **Figure *6***e through **Figure *6***h). MTS and DNA quantification data showed no significant differences between the PLLA/PLLA-BBGs scaffolds and the control experiment. It is also relevant to emphasize that, after 21 days of cell culture a complete monolayer of cells were attached to the outer surface of the scaffolds in all the cases. However, this phenomenon was more pronounced for the PLLA-BBGs scaffolds, in particular for the composite that was formulated with the BBG-Ca microparticles, i.e. PLLA-BBG-Ca (**Figure *6***c). In combination with the bioactivity analysis (where the PLLA-BBG-Ca scaffold presented a higher deposition of calcium phosphate crystalline phases), the biological evaluation data supports the suitability of this composition to generate a 3D porous structure that is able to promote cell attachment, proliferation and

colonization of the bulk of the scaffold [54]. The great biodegradable and bioactive properties of PLLA-BBG composite scaffolds combined with their suitability for cell colonization support that PLLA-BBG composite scaffolds can be used to achieve medical-grade material for development of bone tissue engineered implants. Other *in vivo* mechanical and biocompatibility studies will be done in the near future.

4. Conclusions

PLLA-BBG scaffolds were successfully prepared through the incorporation of 25% (w/w) of BBGs (with different divalent glass modifier cations, i.e. Mg^{2+}, Ca^{2+} and Sr^{2+}) in the PLLA matrix. The µCT analysis demonstrated that our procedure generated 3D scaffolds with an interconnected structured with a high degree of porosity (58 to 62% of interconnectivity and 53 to 67% of porosity) and a mean pore diameter >100 µm - suitable for cell colonization of the bulk of the scaffolds. Degradation studies confirmed that the incorporation of BBG particles enhance the degradability of the composites with a constant release of inorganic species to the surrounding media. Bioactivity studies demonstrated that PLLA-BBG scaffolds are capable to produce a calcium phosphate-rich surface layer (PLLA-BBG-Ca and PLLA-BBG-Sr) after 7 days of culture (Ca/P ratio ~1.7). *In vitro* cell studies revealed that the proposed PLLA-BBG scaffolds do not elicit any cytotoxicity over 7 days of culture, while hASC's were able to adhere and proliferate throughout the surface and inner sections of the porous scaffolds, being a suitable for bone tissue engineering.

Acknowledgments

JSF acknowledges the Portuguese Foundation for Science and Technology (FCT) for his PhD grant BD/73162/2010. This work was partially supported by the European

Research Council grant agreement ERC-2012-ADG20120216-321266 - project ComplexiTE.

References

[1] J. Juhasz, S. Best, J Mater Sci, 47 (2012) 610-624.

[2] P.V. Giannoudis, H. Dinopoulos, E. Tsiridis, Injury, 36 (2005) S20-S27.

[3] Q. Fu, E. Saiz, M.N. Rahaman, A.P. Tomsia, Materials Science and Engineering: C, 31 (2011) 1245-1256.

[4] A. Gantar, L.P. da Silva, J.M. Oliveira, A.P. Marques, V.M. Correlo, S. Novak, R.L. Reis, Materials Science and Engineering: C, 43 (2014) 27-36.

[5] K. Rezwan, Q.Z. Chen, J.J. Blaker, A.R. Boccaccini, Biomaterials, 27 (2006) 3413-3431.

[6] J. Mota, N. Yu, S.G. Caridade, G.M. Luz, M.E. Gomes, R.L. Reis, J.A. Jansen, X.F. Walboomers, J.F. Mano, Acta Biomaterialia, 8 (2012) 4173-4180.

[7] Y. Li, Z.-g. Wu, X.-k. Li, Z. Guo, S.-h. Wu, Y.-q. Zhang, L. Shi, S.-h. Teoh, Y.-c. Liu, Z.-y. Zhang, Biomaterials, 35 (2014) 5647-5659.

[8] A. Hoppe, A.R. Boccaccini, 7 - Bioactive glass foams for tissue engineering applications, in: P.A. Netti (Ed.) Biomedical Foams for Tissue Engineering Applications, Woodhead Publishing, 2014, pp. 191-212.

[9] L.F. Boesel, H.S. Azevedo, R.L. Reis, Biomacromolecules, 7 (2006) 2600-2609.

[10] A.A.A. Barros, A. Alves, C. Nunes, M.A. Coimbra, R.A. Pires, R.L. Reis, Acta Biomaterialia, 9 (2013) 9086-9097.

[11] F.O. Gomes, R.A. Pires, R.L. Reis, Materials Science and Engineering: C, 33 (2013) 1361-1370.

[12] S. Amorim, A. Martins, N.M. Neves, R.L. Reis, R.A. Pires, Journal of Materials Chemistry B, 2 (2014) 6939-6946.

[13] K. Madhavan Nampoothiri, N.R. Nair, R.P. John, Bioresource Technology, 101 (2010) 8493-8501.

[14] H.-Q. Liang, Q.-Y. Wu, L.-S. Wan, X.-J. Huang, Z.-K. Xu, Journal of Membrane Science, 446 (2013) 482-491.

[15] M. Martins, R. Craveiro, A. Paiva, A.R.C. Duarte, R.L. Reis, Chemical Engineering Journal, 241 (2014) 122-130.

[16] A.G. Mikos, Y. Bao, L.G. Cima, D.E. Ingber, J.P. Vacanti, R. Langer, Journal of Biomedical Materials Research, 27 (1993) 183-189.

[17] M. Veysi, G.-P. Daniel, N. Tyler, J.L. John, J.H. Derek, Journal of Micromechanics and Microengineering, 25 (2015) 125001.

[18] A. Hoppe, N.S. Güldal, A.R. Boccaccini, Biomaterials, 32 (2011) 2757-2774.

[19] J. Chakraborty, S. Sengupta, S. Ray, S. Ghosh, R. Kapoor, S.P. Gouri, G. Pande, S. Datta, Surface and Coatings Technology, 240 (2014) 437-443.

[20] S. Labbaf, O. Tsigkou, K.H. Müller, M.M. Stevens, A.E. Porter, J.R. Jones, Biomaterials, 32 (2011) 1010-1018.

[21] T. Okuda, K. Ioku, I. Yonezawa, H. Minagi, G. Kawachi, Y. Gonda, H. Murayama, Y. Shibata, S. Minami, S. Kamihira, H. Kurosawa, T. Ikeda, Biomaterials, 28 (2007) 2612-2621.

[22] M. Rouahi, E. Champion, P. Hardouin, K. Anselme, Biomaterials, 27 (2006) 2829-2844.

[23] N.J. Lakhkar, I.-H. Lee, H.-W. Kim, V. Salih, I.B. Wall, J.C. Knowles, Advanced Drug Delivery Reviews, 65 (2013) 405-420.

[24] T. Uysal, A. Ustdal, M.F. Sonmez, F. Ozturk, The Angle Orthodontist, 79 (2009) 984-990.

[25] Y.C. Fredholm, N. Karpukhina, D.S. Brauer, J.R. Jones, R.V. Law, R.G. Hill, J R Soc Interface, 9 (2012) 880-889.

[26] F. Yang, D. Yang, J. Tu, Q. Zheng, L. Cai, L. Wang, STEM CELLS, 29 (2011) 981-991.

[27] V. Karageorgiou, D. Kaplan, Biomaterials, 26 (2005) 5474-5491.

[28] K. Park, Journal of Controlled Release, 184 (2014) 79.

[29] K. Zhang, Y. Zhang, S. Yan, L. Gong, J. Wang, X. Chen, L. Cui, J. Yin, Acta Biomaterialia, 9 (2013) 7276-7288.

[30] S.F. Hulbert, F.A. Young, R.S. Mathews, J.J. Klawitter, C.D. Talbert, F.H. Stelling, Journal of Biomedical Materials Research, 4 (1970) 433-456.

[31] J.M. Sobral, S.G. Caridade, R.A. Sousa, J.F. Mano, R.L. Reis, Acta Biomaterialia, 7 (2011) 1009-1018.

[32] P. Danilevicius, L. Georgiadi, C.J. Pateman, F. Claeyssens, M. Chatzinikolaidou, M. Farsari, Applied Surface Science.

[33] T. Kokubo, H. Takadama, Biomaterials, 27 (2006) 2907-2915.

[34] Z. Hong, R.L. Reis, J.F. Mano, Acta Biomaterialia, 4 (2008) 1297-1306.

[35] X. Xu, X. Chen, A. Liu, Z. Hong, X. Jing, European Polymer Journal, 43 (2007) 3187-3196.

[36] H. Kaczmarek, M. Nowicki, I. Vuković-Kwiatkowska, S. Nowakowska, J Polym Res, 20 (2013) 1-12.

[37] A.R. Boccaccini, M. Erol, W.J. Stark, D. Mohn, Z. Hong, J.F. Mano, Composites Science and Technology, 70 (2010) 1764-1776.

[38] D.W. Hutmacher, Biomaterials, 21 (2000) 2529-2543.

[39] A.W. Wren, N.M. Cummins, A. Coughlan, M.R. Towler, Journal of Materials Science, 45 (2010) 3554-3562.

[40] I. Armentano, M. Dottori, E. Fortunati, S. Mattioli, J.M. Kenny, Polymer Degradation and Stability, In Press, Corrected Proof (2010).

[41] L.L. Hench, Journal of the American Ceramic Society, 81 (1998) 1705-1728.

[42] D.K. Pattanayak, Materials Science and Engineering: C, 29 (2009) 1709-1714.

[43] K. Zhang, Y. Wang, M.A. Hillmyer, L.F. Francis, Biomaterials, 25 (2004) 2489-2500.

[44] H.H. Lu, A. Tang, S.C. Oh, J.P. Spalazzi, K. Dionisio, Biomaterials, 26 (2005) 6323-6334.

[45] W. Huang, D. Day, K. Kittiratanapiboon, M. Rahaman, Journal of Materials Science: Materials in Medicine, 17 (2006) 583-596.

[46] J. Terra, E.R. Dourado, J.-G. Eon, D.E. Ellis, G. Gonzalez, A.M. Rossi, Physical Chemistry Chemical Physics, 11 (2009) 568-577.

[47] C. Rey, C. Combes, C. Drouet, D. Grossin, 1.111 - Bioactive Ceramics: Physical Chemistry, in: P. Ducheyne (Ed.) Comprehensive Biomaterials, Elsevier, Oxford, 2011, pp. 187-221.

[48] F. Granados-Correa, J. Bonifacio-MartÍNez, J. Serrano-GÓMez, Revista internacional de contaminación ambiental, 26 (2010) 129-134.

[49] J. Jia, H. Zhou, J. Wei, X. Jiang, H. Hua, F. Chen, S. Wei, J.-W. Shin, C. Liu, Journal of The Royal Society Interface, 7 (2010) 1171-1180.

[50] D.d.S. Tavares, C.X. Resende, M.P. Quitan, L.d.O. Castro, J.M. Granjeiro, G.d.A. Soares, Materials Research, 14 (2011) 456-460.

[51] C. Lindahl, H. Engqvist, W. Xia, Applied Surface Science, 266 (2013) 199-204.

[52] Y. Liang, H. Li, J. Xu, X.I.N. Li, X. Li, Y. Yan, M. Qi, M.I.N. Hu, Experimental and Therapeutic Medicine, 9 (2015) 172-176.

[53] P.A. Zuk, M. Zhu, P. Ashjian, D.A. De Ugarte, J.I. Huang, H. Mizuno, Z.C. Alfonso, J.K. Fraser, P. Benhaim, M.H. Hedrick, Molecular Biology of the Cell, 13 (2002) 4279-4295.

[54] J.H. Lee, J.W. Rhie, D.Y. Oh, S.T. Ahn, Biochemical and Biophysical Research Communications, 370 (2008) 456-460.

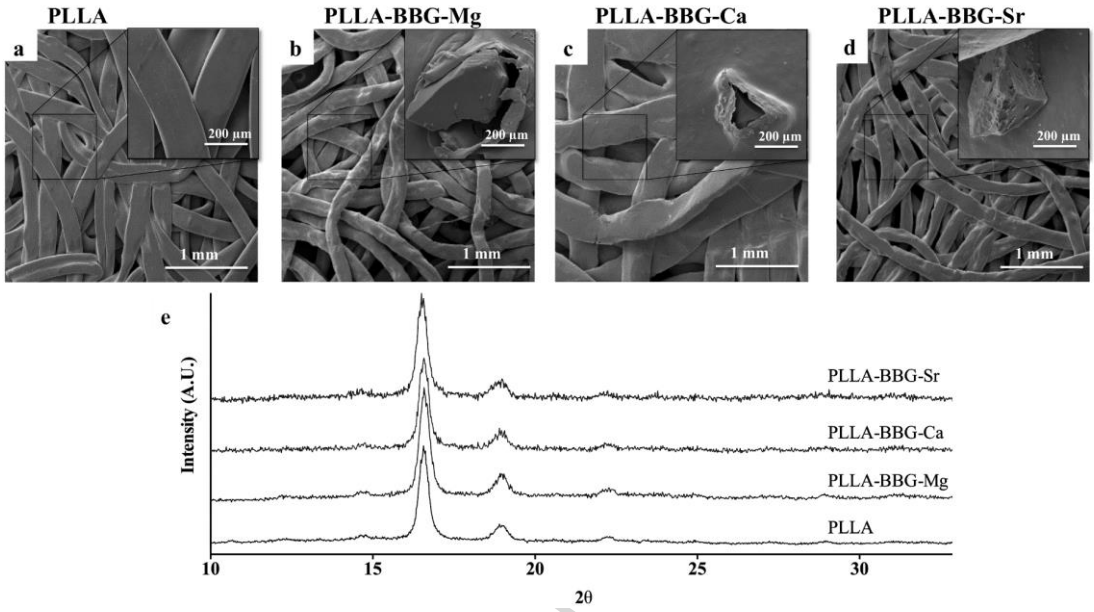

Figure 1

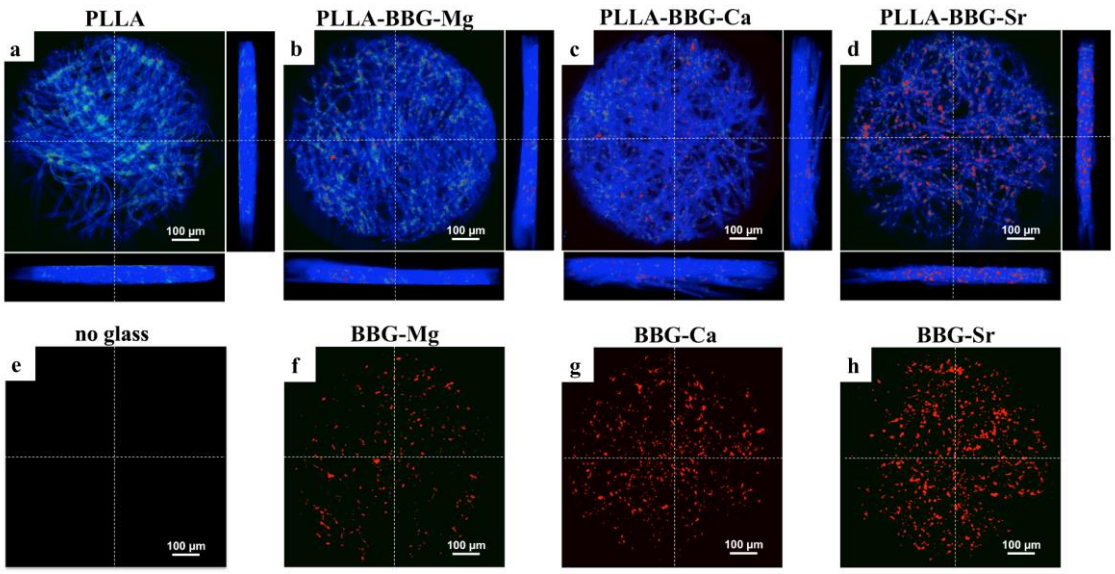

Figure 2

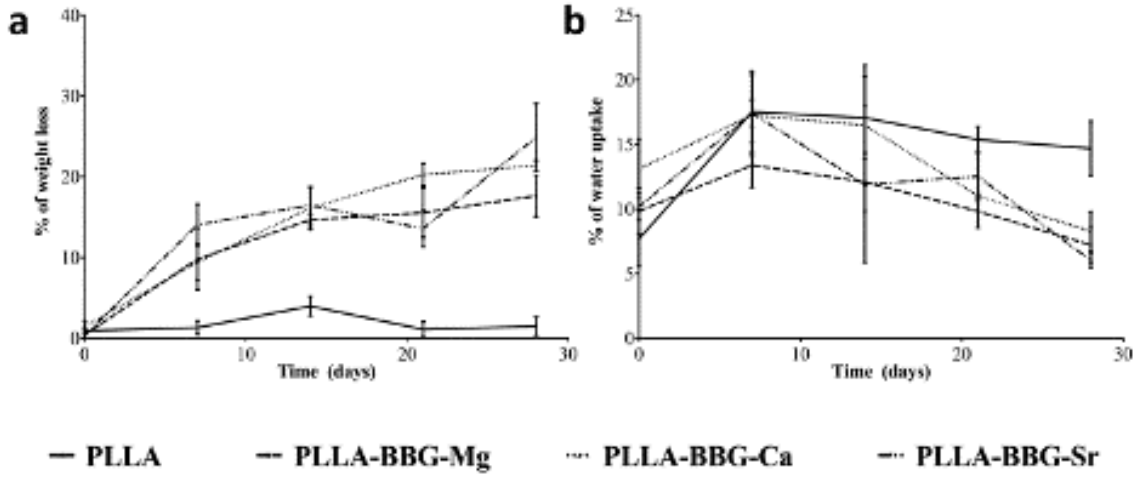

c

PLLA-BBG-Mg	Concentration (μM)		
Time (days)	Mg	Si	B
0	9	5	8
7	168	96	190
14	227	70	244
21	284	121	345
30	357	194	439

PLLA-BBG-Ca	Concentration (μM)		
Time (days)	Ca	Si	B
0	4	6	3
7	31	26	34
14	43	28	60
21	64	36	94
30	72	44	113

PLLA-BBG-Sr	Concentration (μM)		
Time (days)	Sr	Si	B
0	8	8	5
7	48	39	35
14	64	42	60
21	99	30	92
30	105	60	95

Figure 3

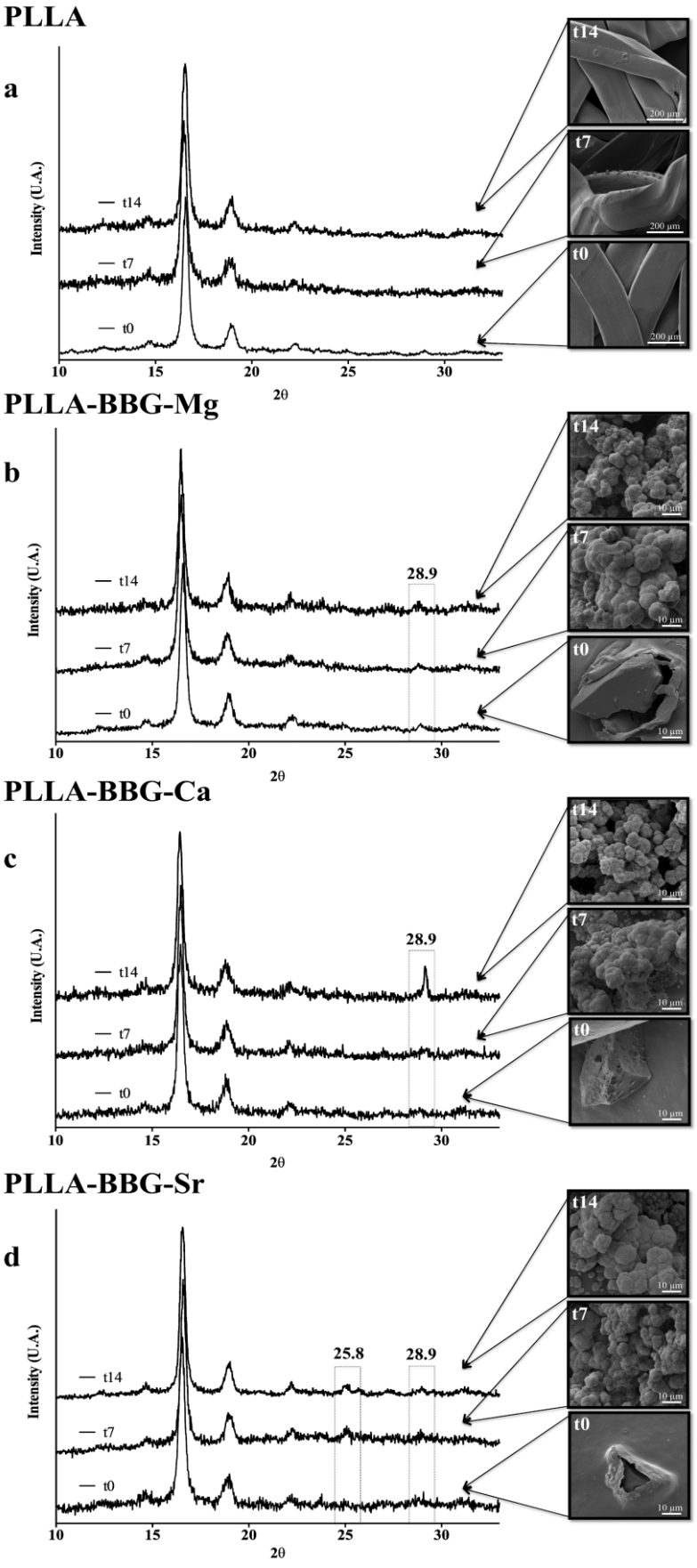

Figure 4

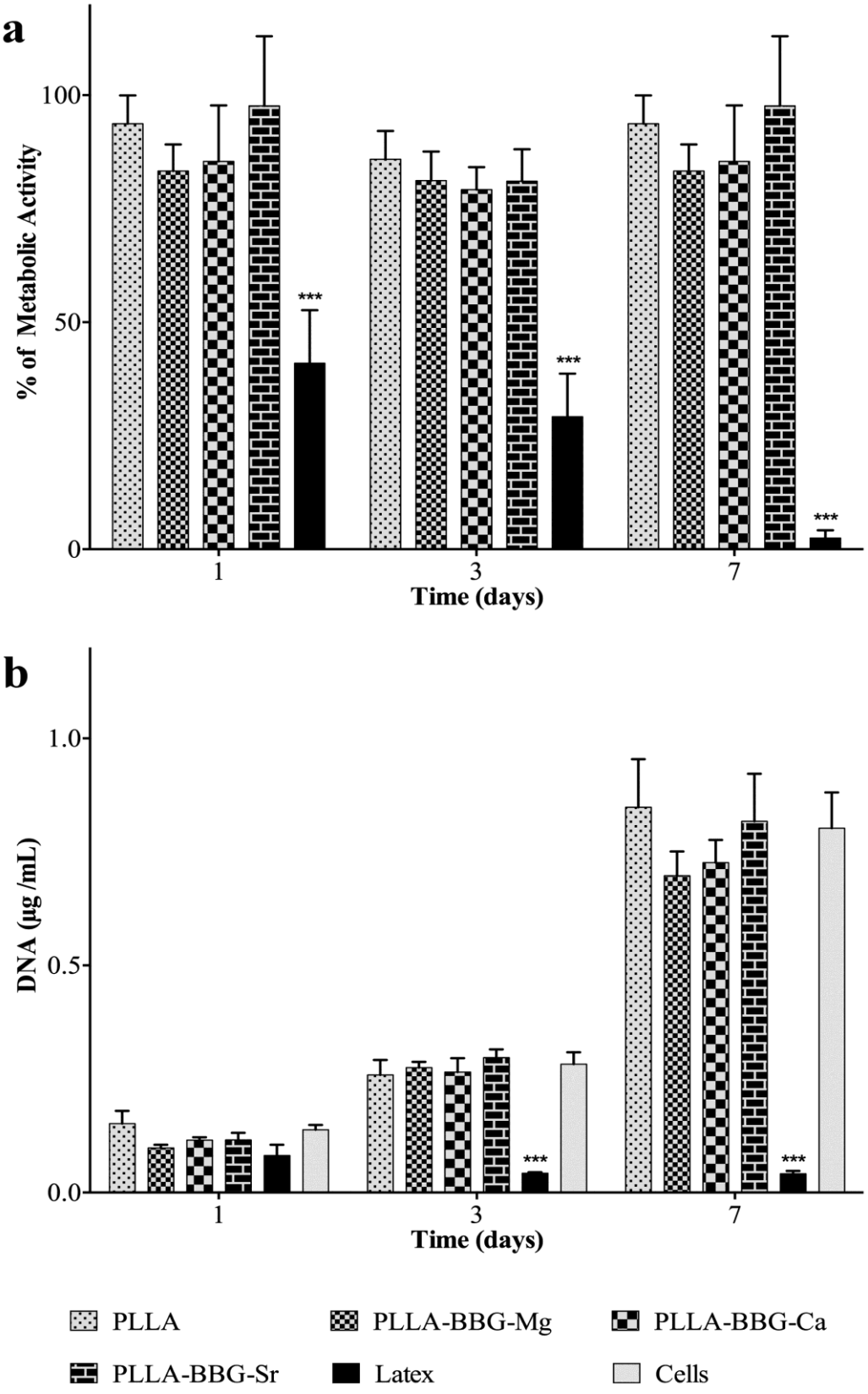

Figure 5

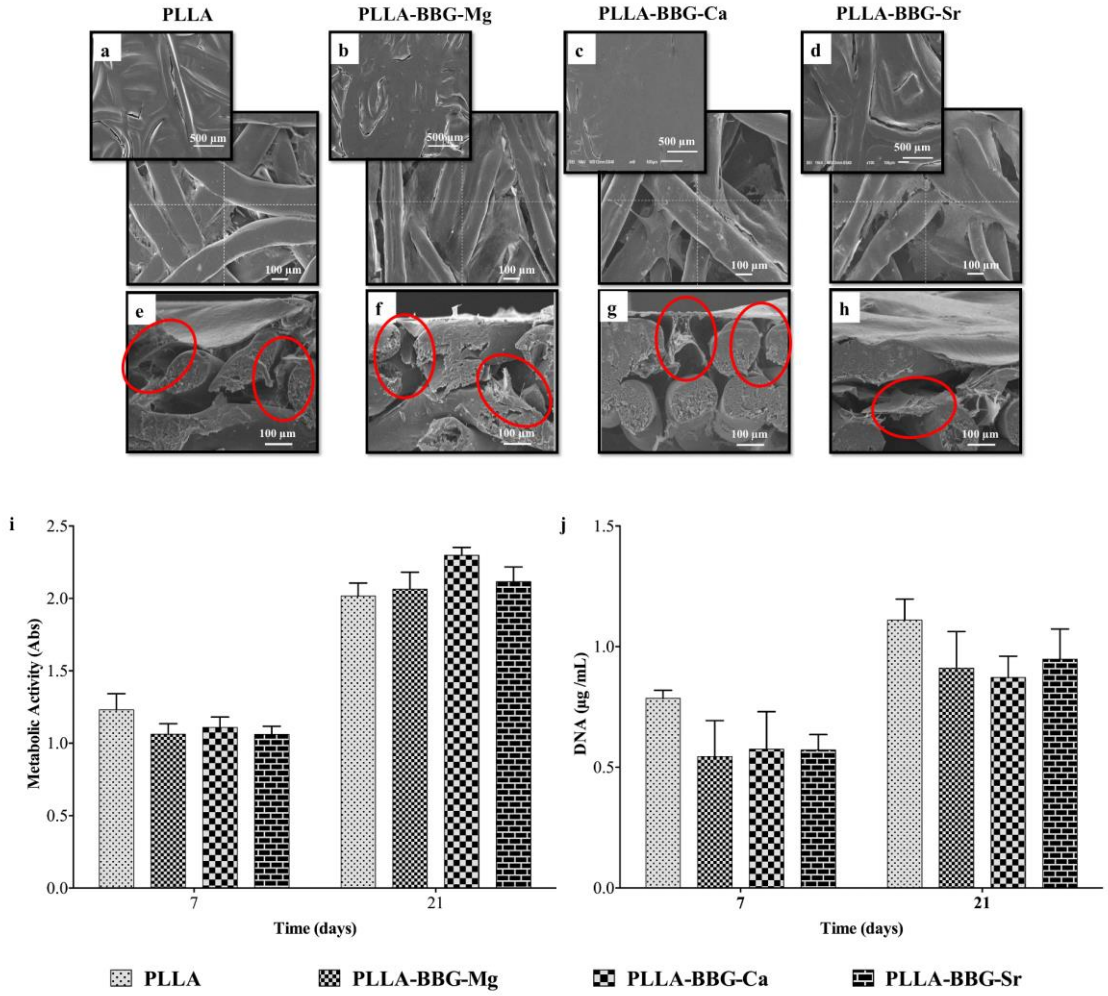

Figure 6

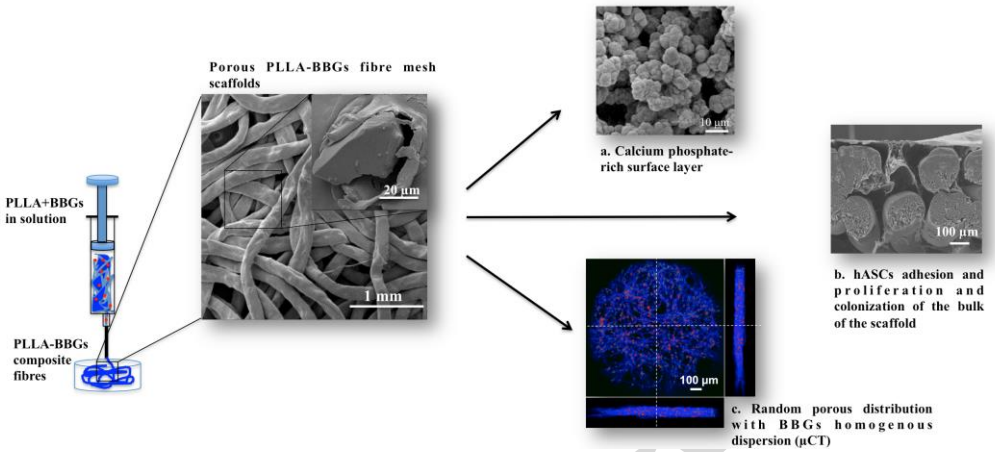

Graphical abstract

Highlights

- We prepared borosilicate glasses and their PLLA composites in the form of fibres
- These glasses imparted bioactivity and controlled degradability to the fibres
- The prepared fibres did not elicit cytotoxicity
- hASCs attached and proliferated in the surface and inner sections of the scaffolds
- The composites present appropriate properties to be used in bone tissue engineering